JOURNAL OF VIROLOGY, June 2006, p. 5199–5210 Vol. 80, No. 11
0022-538X/06/$08.00+0 doi:10.1128/JVI.02723-05

Separate Basic Region Motifs within the Adeno-Associated Virus Capsid Proteins Are Essential for Infectivity and Assembly

Joshua C. Grieger,[1,2] Stephen Snowdy,[1] and Richard J. Samulski[1,2]*

Curriculum in Genetics and Molecular Biology[1] and Gene Therapy Center,[2] University of North Carolina, Chapel Hill, North Carolina 27599

Received 28 December 2005/Accepted 3 March 2006

Adeno-associated virus (AAV) is gaining momentum as a gene therapy vector for human applications. However, there remain impediments to the development of this virus as a vector. One of these is the incomplete understanding of the biology of the virus, including nuclear targeting of the incoming virion during initial infection, as well as assembly of progeny virions from structural components in the nucleus. Toward this end, we have identified four basic regions (BR) on the AAV2 capsid that represent possible nuclear localization sequence (NLS) motifs. Mutagenesis of BR1 (^{120}QAKKRVL^{126}) and BR2 (^{140}PGKKRPV^{146}) had minor effects on viral infectivity (~4- and ~10-fold, respectively), whereas BR3 (^{166}PARKRLN^{172}) and BR4 (^{307}RPKRLN^{312}) were found to be essential for infectivity and virion assembly, respectively. Mutagenesis of BR3, which is located in Vp1 and Vp2 capsid proteins, does not interfere with viral production or trafficking of intact AAV capsids to the nuclear periphery but does inhibit transfer of encapsidated DNA into the nucleus. Substitution of the canine parvovirus NLS rescued the BR3 mutant to wild-type (wt) levels, supporting the role of an AAV NLS motif. In addition, rAAV2 containing a mutant form of BR3 in Vp1 and a wt BR3 in Vp2 was found to be infectious, suggesting that the function of BR3 is redundant between Vp1 and Vp2 and that Vp2 may play a role in infectivity. Mutagenesis of BR4 was found to inhibit virion assembly in the nucleus of transfected cells. This affect was not completely due to the inefficient nuclear import of capsid subunits based on Western blot analysis. In fact, aberrant capsid foci were observed in the cytoplasm of transfected cells, compared to the wild type, suggesting a defect in early viral assembly or trafficking. Using three-dimensional structural analysis, the lysine- and arginine-to-asparagine change disrupts hydrogen bonding between these basic residues and adjacent beta strand glutamine residues that may prevent assembly of intact virions. Taken together, these data support that the BR4 domain is essential for virion assembly. Each BR was also found to be conserved in serotypes 1 to 11, suggesting that these regions are significant and function similarly in each serotype. This study establishes the importance of two BR motifs on the AAV2 capsid that are essential for infectivity and virion assembly.

The mechanisms by which DNA viruses transfer their genomes to the nucleus can follow one of three generalized pathways. One pathway is that the DNA is shuttled into the nucleus by the entire virion, followed by intranuclear uncoating of the virus and release of the viral DNA, as shown for polyomavirus infection (58). Another pathway leading to genome delivery occurs when the virion is unassembled before it reaches the nucleus, and one of the capsid proteins, or some other viral protein, then carries the DNA to the nucleus (e.g., herpes simplex virus type 1 and adenovirus) (14, 39, 50, 54). Under this scenario, a capsid component would either shuttle the DNA into the nucleus or release the DNA at the nuclear pore, allowing the DNA to diffuse across the membrane. A third nuclear entry pathway, used only by some retroviruses, is entering the nucleus during mitosis, when the nuclear membrane becomes fragmented.

During the course of an adeno-associated virus (AAV) infection, the capsid proteins must target the nucleus twice. The first targeting event is during the initial infection when the virus must deliver the viral genome to the nucleus for replication and for transcription of mRNAs that encode replication proteins and progeny virus structural proteins. Since AAV replicates in the nucleus of its host cell (59), the second targeting event occurs when progeny viral capsid subunits enter the nucleus for assembly into progeny virions. Despite the importance of this critical aspect of AAV infection, very little is known of how AAV provides for transport of its genome across the nuclear envelope and how the progeny capsid proteins gain access to the nucleus for genome encapsidation and virion assembly. It is not known whether the virus enters the nucleus intact and is subsequently uncoated in the nucleus or whether the virus is uncoated in the cytoplasmic compartment. What is known, however, is that genome entry into the nucleus is inefficient (35, 64).

The viral capsid measures approximately 25 nm in diameter and is composed of three proteins termed Vp1, Vp2, and Vp3, which are translated from the same open reading frame but from differential splicing (Vp1) and alternative translational start sites (Vp2 and Vp3, respectively). Therefore, the capsid proteins are identical in their C termini. Together, these proteins form the viral capsid shell in a stoichiometric ratio of 1:1:10. Vp3 is the most abundant subunit in the virion and is used for receptor recognition at the surface of cells defining the tropism of AAV. A phospholipase domain, essential for viral infectivity, has been identified in the unique N terminus of

* Corresponding author. Mailing address: Gene Therapy Center, University of North Carolina at Chapel Hill, 7119 Thurston Bowles, CB 7352, Chapel Hill, NC 27599-7352. Phone: (919) 962-1224. Fax: (919) 966-0907. E-mail: rjs@med.unc.edu.

Vp1 (13, 68). The functional significance of Vp2 remains ambiguous, but recent studies have shown that it is possible to make viable virus lacking Vp2 in a recombinant background (15, 57).

Surprisingly, a nuclear localization sequence (NLS) was previously identified within the Vp2 N terminus of AAV2 and was proposed as a mediator for targeting individual capsid proteins to the nucleus during progeny virion assembly (22). NLSs are usually concentrated in basic residues, tend to be hydrophilic, and are preceded by β-turn/random coil regions (17, 24). NLS regions have also been identified on other parvoviruses, such as canine parvovirus (CPV) and minute virus of mice (MVM). It was found that when a basic sequence representing a putative NLS in VP1 of CPV was conjugated to bovine serum albumin (BSA) and subsequently microinjected into HeLa cells, the BSA localized to the nucleus (56). It was further demonstrated that microinjection of antibodies to the basic region (BR) into the cytoplasm of cells was sufficient to prevent subsequent infection of the cells by CPV. The sequence identified as the NLS of CPV was PAKRARRG, which is similar to that identified for AAV2 (PARKRLNF) (55). MVM has been shown to contain multiple NLSs within its capsid that act at different times during its infectious cycle (32, 33). Lombardo et al. identified several BRs on the capsid and found that the sequence ^{528}KGKLTMRAKLR^{538} is necessary for the localization of the major capsid protein to the nucleus and that VP1 relies upon VP2 for cotransport across the nuclear envelope. Once establishing the sequence necessary for the nuclear uptake of viral capsid proteins during viral assembly, Lombardo et al. found other BRs within the MVM capsid that conferred infectivity upon the virus, possibly by targeting the incoming virion to the nucleus of the target host. Interestingly, all of the BRs identified were on the inside of the virion, indicating that the virus must undergo some conformational change once inside the cell in order to complete the infection.

Although one NLS (BR3) on the Vp2 N terminus was identified by fusing truncated forms of Vp2 to green fluorescent protein (GFP), the mechanism through which the AAV virion gains access to the nuclear interior of its host cell remains largely unknown. In the present study we set out to identify all BRs within AAV's capsid proteins that resemble NLSs. The program P-SORT was used to search the AAV2 capsid sequence for NLS-like regions. Four BRs were identified and, respectively, named BR1 through BR4, as depicted in Fig. 1A. We illustrate here that all of the BRs affect an aspect of the AAV life cycle. BR1 and BR2 mutants were found to play a minor role in infectivity, inhibiting transduction ~4- and ~10-fold, respectively. However, BR3 mutant capsids assembled into intact virions but were defective for transduction in cell lines. The BR4 motif was found to be essential for virion assembly. A more thorough understanding of AAV's nuclear transport mechanisms and how they relate to classical protein import pathways may result in a better understanding of primary steps in AAV infection that have direct impact on vector development.

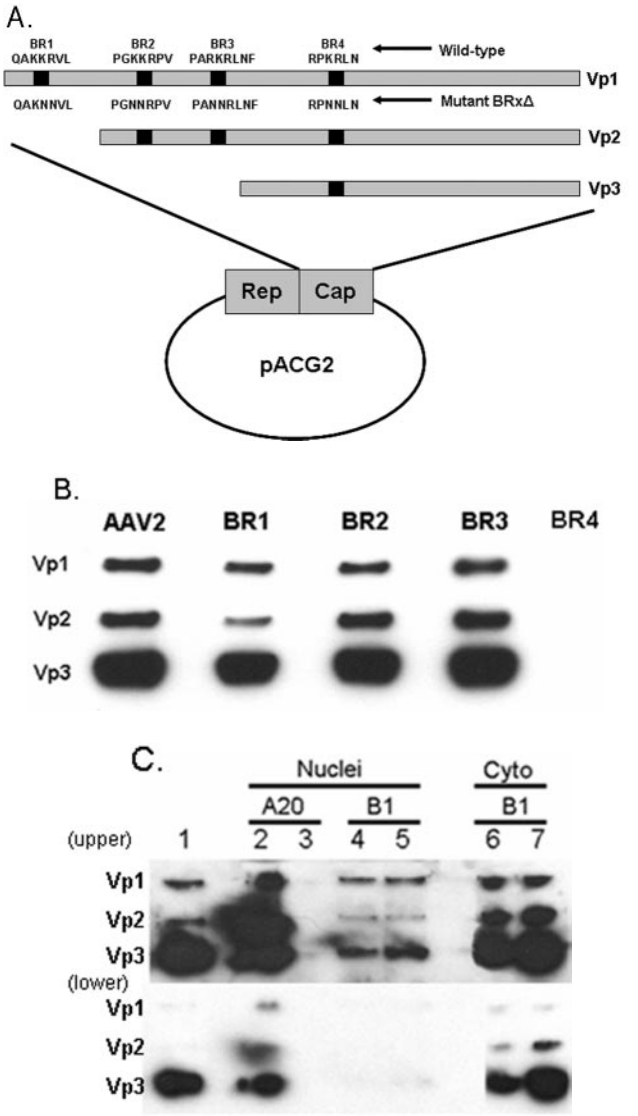

FIG. 1. (A) Schematic of the identified BRs in the AAV capsid gene. A description of the four mutated BRs is portrayed in the schematic. (B) Western blot of AAV2 produced from each of the BR mutant helper plasmids. At 24 h posttransfection, the lysates were centrifuged through an iodixanol step gradient, followed by heparin column purification. Approximately equal titers of purified virus were added to each lane and detected by the B1 antibody. (C) Western blot of the B1 and A20 immunoprecipitations from nuclear (lanes 2 to 5) and cytoplasmic (lanes 6 and 7) fractions of pACG2-wt (lanes 1, 2, 4, and 6) and pACG2-BR4Δ (lanes 3, 5, and 7) transfected 293 cells 24 h posttransfection. Two exposures are presented (the upper exposure is four times longer) to clearly identify capsid proteins after B1 immunoprecipitation in the nucleus.

MATERIALS AND METHODS

Cell culture. HEK293 cells and HeLa cells (American Type Tissue Culture) were maintained at 37°C in Dulbecco modified Eagle medium (Sigma) supplemented with 5% CO_2, 10% fetal bovine serum (Sigma), 100 U of penicillin/ml, and 100 U of streptomycin/ml.

Viral production. Confluent 293 cells were split 1:3 24 h prior to transfection. Triple transfections with pACG2 (31), pTrufEGFP (16), and pXX6-80 (adenovirus helper plasmid) were carried out by calcium phosphate precipitation as previously described (16a). At 48 h posttransfection, cells were scraped, pelleted, and resuspended in phosphate-buffered saline (PBS). rAAV2 was purified by using iodixanol and heparin columns as previously described (69).

Dot blot analysis for determining virus titers. The recovery of virus in terms of genome copies was determined by DNA hybridization. A total of 10 μl of each

sample was incubated in 100 μl of DNase I digestion buffer (10 mM Tris [pH 7.5], 10 mM $MgCl_2$ and 50 U of DNase I/ml), followed by incubation at 37°C for 1 h. The DNase digestion was stopped by addition of 4 μl of 0.5 M EDTA. Then, 120 μl of proteinase K solution (1 M NaCl, 100 μg of proteinase K/ml, 1% Sarkosyl) was added, followed by incubation at 50°C for 2 h. Next, 250 μl of phenol-chloroform was added to the digestion mixture, followed by mixing and centrifugation at 16,000 × *g* for 5 min. To precipitate viral DNA, 1 μl of 20 mg of glycogen/ml, 62.5 μl of 10 M ammonium acetate, and 2.5 volumes of 100% ethanol was added to the aqueous phase. Samples were placed on dry ice for 1 h, followed by centrifugation at 16,000 × *g* for 20 min to pellet the viral DNA. The DNA pellet was then resuspended in 200 μl of Tris-EDTA. After digestion with 0.5 M NaOH for 10 min, aliquots of the samples were applied to a dot blot manifold. The denatured viral DNA was then blotted onto a nylon membrane and probed with a ^{32}P-labeled probe against eGFP.

Site-specific mutagenesis. Mutations to pACG2 were carried out by PCR using the Stratagene Multi-Site-Directed Mutagenesis Kit according to manufacturer's instructions. As depicted in Fig. 1, Lys123 and Arg124 in BR1, Lys143 and Arg144 in BR2, Arg168 and Lys169 in BR3, and Lys604 and Arg605 in BR4 were mutated to Asn to abrogate possible NLS functions. The plasmids expressing only Vp1 or only Vp3 were produced via mutagenesis of the start codons of Vp2/Vp3- and Vp1/Vp2-expressing plasmids, respectively. Mutagenesis of the first three start codons of Vp3 (Met 203, 211, and 235) was essential in order to inhibit its expression Cycling parameters were as follows: 95°C for 1 min (1 cycle), 95°C for 1 min (30 cycles), 55°C for 1 min (30 cycles), and 65°C for 15 min (30 cycles). PCR products were digested with DpnI and used to transform electrocompetent XL10 Gold cells (Stratagene), which were then selected for plasmid uptake by growth on ampicillin selection plates. Colonies were picked and grown overnight in LB growth media, and plasmids isolated by QIAGEN Miniprep kits. Mutations were verified by sequencing of the plasmids utilizing the UNC-CH Automated DNA Sequencing Facility on a 3100 Genetic Analyzer (Applied Biosystems). After sequence verification, each clone was subcloned into the parent plasmid pACG2.

Immunoprecipitations. We transfected 10-cm plates as described above for viral production. Cells were lysed 24 h later by hypotonic swelling and Dounce homogenization in 500 μl of hypotonic buffer, and the nuclei were separated from the cytoplasmic supernatant by centrifugation. The cytoplasmic fraction was made isotonic with 0.11 volumes of 1 M Tris-buffered saline (TBS) and centrifuged at 10,000 × *g* to clear the sample of cytoplasmic debris. The nuclear pellet was washed several times to prevent cytoplasmic protein contamination before resuspension in 100 μl of high-salt buffer, drawn several times through a small-bore needle, and centrifuged at 10,000 × *g* to clear the sample of nuclear debris. The sample was brought to 500 μl by the addition of 1× TBS. A total of 40 μl of either B1 or A20 hybridoma supernatant was added to the samples, and the samples were tumbled overnight at 4°C. Then, 40 μl of protein A/G beads was added to the samples, and the beads were collected by centrifugation at 500 × *g*. Beads were washed three times in radioimmunoprecipitation assay buffer and then subjected to sodium dodecyl sulfate-polyacrylamide gel electrophoresis and Western blotting for the analysis of capsid proteins as described below.

Western blotting. Samples from cell homogenate and purified vector were loaded onto NuPage 10% Bis-Tris gels and run using 1× NuPage MOPS buffer. The XCell SureLock Mini Cell (Invitrogen) was used for electrophoresis. Protein was then transferred to a Hybond ECL membrane utilizing the XCell II Blot module (Invitrogen) for wet transfer according to the manufacturer's protocol for Bis-Tris gels. Each membrane was blocked for 1 h at room temperature using 1× TBS (pH 7.5), 0.1% Tween, and 10% nonfat dry milk (NFDM). The primary B1 antibody was then diluted 1:10 in 1× TBS (pH 7.5), 0.1% Tween, and 2% NFDM, followed by incubation on the membrane for 1 h at room temperature or overnight at 4°C. Excess primary antibody was then washed from the membrane using 1× TBS (pH 7.5)–0.1% Tween four times for 5 min each time. Secondary antibody was then diluted 1:10,000 in 1× TBS (pH 7.5), 0.1% Tween, and 2% NFDM, followed by incubation on the membrane for 1 h at room temperature. Excess secondary was then washed from the membrane as previously described. SuperSignal West Femto Maximum Sensitivity Substrate (Pierce) was then added to each membrane according to the manufacturer's protocol. Each membrane was then exposed to Kodak BioMax MR film.

Transduction experiments. Transduction experiments were carried out utilizing HeLa cells. To keep consistency throughout experiments in the study, HeLa cells were infected with ~3,000 viral genomes/cell. Transduction of HeLa cells was assayed by utilizing a fluorescence microscope at 48 h postinfection.

Immunohistochemistry by TSA. Immunohistochemistry was performed by tyramide system amplification (TSA; Perkin-Elmer) according to manufacturer's instructions with modifications. HeLa cells were seeded onto two-chamber glass slides at 5×10^4 cells/well. After 24 h, cells were infected with ~3,000 physical particles per cell at 4°C for 1 h, washed, and placed at 37°C. After the indicated amount of time, the cells were fixed and permeabilized in 100% methanol at −20°C for 10 min and then washed three times for 5 min each time in room temperature PBS. Cells were blocked in TSA blocking buffer for 1 h at room temperature. Cells were then incubated with monoclonal antibody (MAb) B1 diluted 1:200 in PBS-Tween (PBS-T; PBS with 0.05% Tween). Cells were washed in PBS-T three times for 5 min each time and incubated for 1 h with the secondary antibody (horseradish peroxidase-conjugated rabbit anti-mouse antibody; Sigma) diluted 1:5,000 in PBS-T. Cells were again washed three times for 5 min each time in PBS-T, incubated for 10 min in Tyramide-Cy3 labeling solution, and washed three times for 5 min each time in PBS-T (in light-protected Coplin jar). Two drops of antifade mounting media containing DAPI (4′,6′-diamidino-2-phenylindole; Vecta Shield) was placed on the slide, and a slide cover was sealed onto the slide with nail polish. Slides were imaged immediately by confocal microscopy on a Leica SP2 scanning confocal microscope capable of differential interference contrast overlay.

Fluorescence in situ hybridization by TSA. Fluorescent in situ hybridization was carried out by TSA in accordance with the manufacturer's instructions with modifications (Perkin-Elmer). HeLa cells were seeded onto two-chambered slides at a density of 5×10^4 cells/well. The cells were infected 24 h later by ~3,000 AAV2 particles/cell (or mutants of AAV2) as described above (4°C for 1 h, followed by washing with PBS, and placement at 37°C). After the indicated incubation times, cells were washed four times with PBS and fixed in cold methanol-acetic acid (3:1) for 5 min at −20°C. Cells were then washed three times for 5 min each time in PBS. Dehydration of the cells was carried out by 2-min incubations in each of 70% ethanol at −20°C, 90% ethanol at room temperature, and 100% ethanol at room temperature. Slides were then treated with protease at 100 μg/ml in PBS for 60 min at 37°C and again dehydrated as described above. Cells were then incubated in 50% formamide–2×SSC (1× SSC is 0.15 M NaCl plus 0.015 M sodium citrate) for 5 min at 72°C.

Preparation of DNA probe. GFP gene DNA was labeled with biotin (Boerhinger Biotin NT) according to the manufacturer's instructions. The probe solution was made with 10 ng of biotinylated DNA/μl, 15 ng of salmon sperm DNA/μl, 50% formamide, 7% dextran sulfate, and 0.75× SSC. Probe solution was boiled for 10 min and placed onto the cells, and the cells were covered with slide covers and then sealed with rubber cement. Incubation of the cells with the biotinylated probe was carried out overnight at 37°C. After overnight incubation, cells were washed three times for 5 min each time in 50% formamide–2× SSC at 42°C and then washed in PBS-T three times for 5 min each time. Streptavidin-horseradish peroxidase was diluted 1:100 in PBS-T and placed on the cells. Cells were then washed three times for 5 min each time in PBS-T and incubated for 30 min in Tyramide-Cy3 labeling solution. Cells were washed three times for 5 min each time in PBS-T. Two drops of Vecta Shield antifade mounting media was placed on each slide, the cells were covered with a coverslip, and the coverslip was sealed to the slide with rubber cement. Visualization of the sample was carried out on a Leica SP2 scanning confocal microscope.

Confocal immunofluorescence. HeLa cells were seeded at a density of 3×10^4 cells per well for each slide (Nalge Nunc International Lab-Tek II eight-well RS glass slide). HeLa cells were then infected with 300 viral genomes of wild-type AAV2 (wtAAV2)/cell and an adenovirus multiplicity of infection (MOI) of 5 or transfected with 130 ng of XX680, 100 ng of pACG2 or pACG2-BR4Δ, and 65 ng of TR plasmid cytomegalovirus-luciferase and incubated for 24, 18, and 12 h. Cells were then washed three times with 1× PBS, followed by fixing in 1:1 methanol-acetone at room temperature for 5 min. The slides were then air dried briefly and then rehydrated with 1× PBS with 1.5 mM $MgCl_2$ at room temperature for 5 min. The rehydrated cells were then washed two times for 5 min in immunofluorescence (IF) wash buffer (20 mM Tris-HCl [pH 7.6], 137 mM NaCl, 3 mM KCl, 1.5 mM $MgCl_2$, 5 mg of BSA/ml, and 0.05% Tween 20). Primary antibody B1 (1:10) and anti-fibrillarin (1:100) was diluted in IF wash buffer and incubated for 1 h at 37°C. Cells were then washed with IF wash buffer several times for 15 min at room temperature. Secondary anti-mouse (Alexa-Fluor 488) and anti-rabbit (Alexa-Fluor 568) antibodies (Molecular Probes) were then diluted 1:1,000 in IF wash buffer and incubated on the cells for 1 h at 37°C. The cells were then washed as previously described, and mounting media containing DAPI was added to each slide. Samples were viewed on Leica SP2 aobs confocal microscope.

Luciferase assay. Assays of luciferase activity were carried out in accordance with the manufacturer's instructions (Promega), without modification. The luciferase activity was measured by a Tropix TR717 automated plate reader.

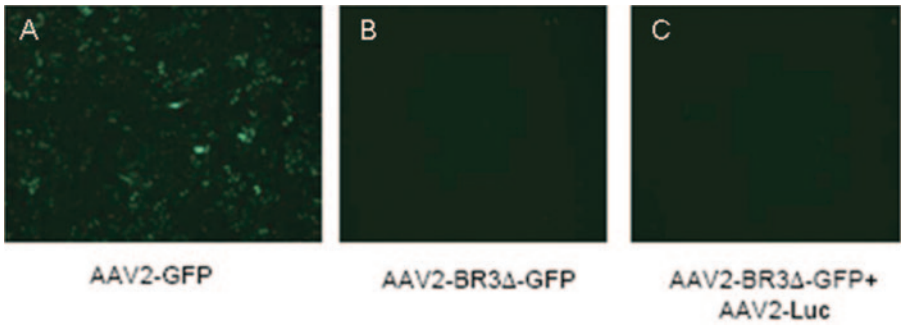

FIG. 2. Fluorescence microscopy images of AAV2, AAV2-BR3Δ-GFP, and coinfection with AAV2-luciferase for a complementation study. HeLa cells were infected with 3,000 viral genomes/cell of AAV2-GFP (A) or AAV2-BR3Δ-GFP (B) and coinfected with AAV2-BR3Δ-GFP and AAV2-Luc (C). Positive cells express GFP. Images were obtained with a Leitz DMIL fluorescence microscope.

RESULTS

Initial characterization of the BRs within the AAV2 capsid. The program P-SORT was used to search the AAV2 capsid sequence for areas concentrated in basic residues. Four regions were identified and named BR1 through BR4 as depicted in Fig. 1A. To establish whether each BR is critical to the life cycle of AAV2, mutagenesis of two of the basic residues in each region to asparagines was carried out as described in Materials and Methods. Basic arginine and lysine residues were replaced with polar and neutral asparagine residues rather than with hydrophobic alanine residues to guarantee that each of the mutagenized BRs had a similar hydropathy to wt while inhibiting possible NLS activity (12, 33, 47). It has been shown in a previous alanine scanning mutagenesis study on the AAV2 capsid that mutagenesis of BR1 to -3 negatively affected infectivity (2 to 3 logs) (62). However, in our study BR1 and BR2 were not found to affect infectivity by 2 to 3 logs but 4- to 10-fold, and we believe this is due to substituting asparagines into each BR as opposed to alanines, which is a more dramatic residue change. As an initial step in characterizing the mutants, we produced recombinant virus by using the previously described pACG2 helper plasmid and assayed for particle titer (ability to protect its viral genome from DNase digestion) and for infectivity (the ability of AAV to deliver the eGFP transgene to the nucleus). All of the experiments carried out here were repeated several times to ensure confidence in the data. It is important to note that the data described here concurs with unpublished data (from the laboratory of Jurgen Kleinschmidt as presented at the International Parvovirus Meeting, 2004).

From these analyses, we defined three phenotypes that fell into three classes. Class 1 mutants produced DNase-resistant particle titers similar to that of rAAV assembled from wt capsids with the correct subunit ratio (Fig. 1B) but transduced cultured HeLa cells less efficiently than wt (data not shown). AAV2-BR1Δ and AAV2-BR2Δ could be categorized as class 1 mutants in that they transduced cells 4- and 10-fold less efficiently than the wt, respectively. A similar study using a different amino acid substitution resulted in a more severe phenotype (62). However, using an amino acid substitution that specifically disrupts potential NLS activity without major changes to hydropathy suggests that these regions do not play the primary role in AAV infectivity in vitro and are not involved in capsid subunit transport into the nucleus for assembly. Class 2 mutants produced DNase-resistant particle titers similar to recombinant virus made from wt capsid proteins but were defective at transducing cultured HeLa cells (Fig. 2B). AAV2-BR3Δ were class 2 mutants. Finally, class 3 mutants did not yield intact vector particles. AAV2-BR4Δ were class 3. Upon further analysis, we found that the BR4Δ mutation inhibited capsid assembly in the nucleus but did not affect nuclear import of capsid subunits (Fig. 1C, lanes 3 and 5).

BR3 plays a role in virion infectivity. The BR3 sequence was previously proposed as a mediator for targeting individual capsid proteins to the nucleus during progeny virion assembly (22). In these experiments, the authors constructed a fusion protein with Vp2 and GFP. The fusion protein localized primarily to the nucleus, but when N-terminal deletions were made to VP2, a BR (denoted BR3 in our study) was found to be necessary for localizing the fusion protein to the nucleus. The authors concluded that Vp2 is necessary for nuclear transfer of the capsid proteins prior to virion assembly. Our data suggest that BR3 is not necessary for the accumulation of capsid proteins during virion production but is instead required for initial virion nuclear targeting and infectivity (Fig. 2). To help support this divergence in the role of BR3 in the AAV life cycle, we carried out additional studies with intact virions carrying the BR3 mutant. Since this virus has wt heparin sulfate (HS) binding activity and can compete for HS binding (data not shown), we determined whether this mutant virus was capable of competing with wt capsids for trafficking events subsequent to initial viral binding to the cell surface. For example, it has been suggested that AAV is internalized into endosomes at a ratio of 1 viral particle per endosome (49). However, it is unlikely that the endosomes containing AAV traffic all of the way to the nucleus without merging with other AAV-containing endosomes, since endosomal merging is part of the normal endosome trafficking mechanism in mammalian cells (30). To test this aspect of AAV trafficking, wt capsids with a luciferase transgene (AAV2-Luc) were allowed to bind HeLa cells at 4°C, followed by the addition of wtAAV2-GFP or AAV2-BR3Δ-GFP to the cell supernatant, and warmed to 37°C, and the luciferase activity was measured 12 h later. wtAAV2-GFP and AAV2-BR3Δ-GFP competed with the wtAAV2-Luc at a step subsequent to receptor binding and, in turn, reduced the expression of the wtAAV2-Luc by more than 50% (data not shown). In addition to determining that AAV2-BR3Δ would compete with wtAAV trafficking, we asked the

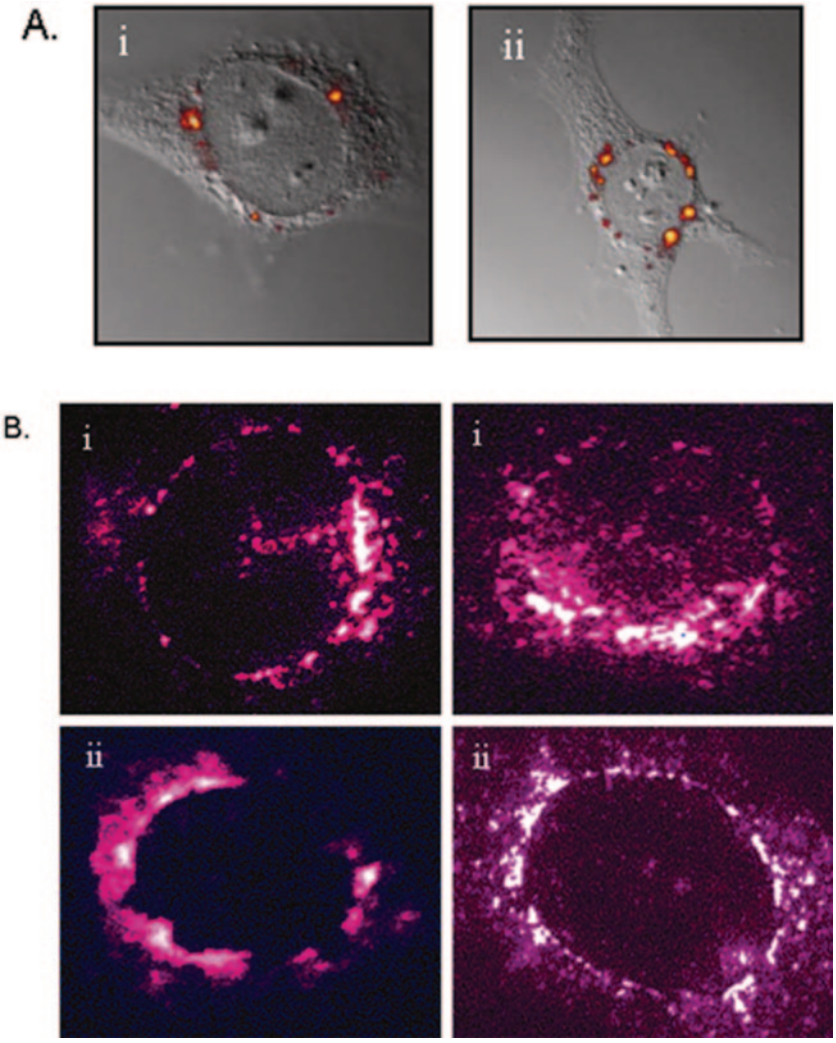

FIG. 3. Confocal microscopy images of the subcellular localization of AAV2 and AAV2-BR3Δ capsid proteins (A) or fluorescent in situ hybridization against the GFP gene after infection of HeLa cells (B). HeLa cells were grown in chambered glass slides and infected with either AAV2-GFP (i) or AAV2-BR3Δ-GFP (ii). Cells were processed 24 h later for immunohistochemistry with the MAb B1 and fluorescence in situ hybridization for the GFP genomes. The samples were then processed by using TSA. (B) Two cells were selected from a population of cells to illustrate the low concentration (left panels) and high concentration (right panels) of GFP genomes in the nucleus. The red staining represents capsid protein (A) and GFP genomes (B).

reciprocal question: could wtAAV particles facilitate AAV2-BR3Δ productive infection and rescue the mutant phenotype? We reasoned that if transduction by the AAV2-BR3Δ virus was blocked by an inability of the virus to carry out a specific trafficking step (i.e., endosome escape), maybe coinfection with nondefective virions would allow the AAV2-BR3Δ-GFP to transduce cells. HeLa cells in culture were infected simultaneously with AAV2-Luc and AAV2-BR3Δ-GFP and assayed 48 h later by fluorescence microscopy for GFP expression. Figure 2C depicts that coinfection of HeLa cells with AAV2-Luc and AAV2-BR3Δ-GFP does not rescue the infectivity of the BR3Δ mutant virus. Based on the present understanding of AAV infection, these data suggest that the mutation may affect a trafficking step downstream of endosome escape.

Tracking AAV2-BR3Δ mutant via confocal microscopy. Previous methods of detecting AAV capsid proteins in tissue culture cells required MOIs of 1 million virions per cell. We established a protocol through which only 1,000 to 5,000 particles are needed per cell to image the capsid proteins by immunohistochemistry, since 1 million particles per cell (and perhaps even 5,000 particles per cell) is in excess of physiological levels. We optimized the TSA (Bio-Rad) protocol for detecting AAV capsid proteins in HeLa cells cultured in chambered glass slides (see Materials and Methods) and viewed the capsid proteins by confocal microscopy. The HeLa cells were infected for 24 h with 3,000 viral genomes of wtAAV2-GFP or AAV2-BR3Δ-GFP per cell, processed for TSA-based immunohistochemistry, and assayed by confocal fluorescence microscopy. The location of AAV capsid proteins for both AAV2-GFP and AAV2-BR3Δ-GFP (red staining) utilizing the B1 antibody shows capsid proteins accumulating in the perinuclear region (Fig. 3Ai and ii) similar to published data (1, 35, 64). Therefore, AAV2-BR3Δ-GFP was internalized normally

FIG. 4. Fluorescence microscopy images of AAV2-infected HeLa cells. Substitution of the canine parvovirus NLS for the BR3Δ mutant sequence rescues transduction. HeLa cells were infected with 3,000 viral genomes/cell of AAV2-GFP (A), AAV2-BR3Δ-GFP (B), and AAV2-CPVNLS-GFP (C). Positive cells express GFP. Images were obtained with a Leitz DMIL fluorescence microscope.

and accumulated at the nuclear periphery similarly to wtAAV2-GFP.

Once we established that AAV2-BR3Δ traffics to the nuclear periphery similarly to AAV2, we sought to determine whether the associated viral genome entered the nucleus. HeLa cells were infected with AAV2-GFP or AAV2-BR3Δ-GFP and processed 24 h later for fluorescence in situ hybridization for the incoming GFP genome. Cells were then examined by confocal microscopy to determine the location of the GFP gene delivered by the incoming virions. Clear punctate staining can be seen inside the nucleus for wtAAV2-GFP-infected cells (Fig.3Bi), with the majority of the viral genomes located in a rim around the nucleus, as was previously shown for the capsid proteins (Fig. 3A) (1, 35, 64). However, a majority of the staining for the GFP gene, delivered by the BR3Δ vector, was located around the perimeter of the nucleus with very little, if any, GFP genomes in the nucleus (Fig.3Bii). These data strongly suggest that the AAV2-BR3Δ mutant is incapable of delivering its genome into the nucleus with an efficiency similar to wtAAV2 capsids and provide a working explanation for the inability of this mutant virion to transduce target cells.

Use of a heterologous NLS to rescue infectivity. Although the studies described above support the role of NLS activity for BR3, substitution experiments with a known NLS motif were carried out to further establish this hypothesis. PCR site-directed mutagenesis was used to replace the BR3Δ mutation in pACG2-BR3Δ with the nuclear localization motif (NLS) identified for CPV, PAKRARR (55, 56). Figure 4 shows HeLa cells 24 h postinfection with wtAAV2-GFP (Fig. 4A), AAV2-BR3Δ-GFP (Fig. 4B), or AAV2-CPVNLS-GFP (Fig. 4C). Substitution of the NLS of CPV restored infectivity to the AAV2-BR3Δ-GFP mutant as shown by the GFP-expressing cells in panel C. The NLS identified within CPV was capable of substituting the function provided by the AAV2 putative NLS (BR3), providing independent evidence that the primary role of BR3 is transport of viral genomes, not capsid subunits as previously proposed (22), to the nucleus.

BR3 is functional in both Vp1 and Vp2 capsid proteins. Since AAV2 BR3 is located in both Vp1 and in Vp2 and a previously published study has suggested that Vp2 is dispensable (57), we sought to determine whether the function provided by BR3 is derived solely from Vp1 or Vp2. Previously, the ability to express AAV capsid proteins using separate helper plasmids has allowed one to systematically determine the role of each subunit in AAV infection (57). Toward this end, we produced virions composed of Vp3 only, Vp1/Vp3, Vp1BR3Δ/Vp3, Vp2/Vp3, and Vp1BR3Δ/Vp2/Vp3 packaging the GFP transgene. HeLa cells were infected with 3,000 viral genomes/cell of each vector both in the presence (Fig. 5A) and in the absence (data not shown) of adenovirus (MOI of 5). Infectivity was assessed by fluorescence microscopy to identify GFP fluorescing cells. As previously described (13, 45), Vp3 only and Vp2/Vp3 virions were not infectious (Fig. 5Aii and 5Aiii) due to the lack of the phospholipase domain. Upon the addition of wtVp1, the Vp1/Vp3 and Vp1/Vp2/Vp3 viruses were found to be infectious (Fig. 5Aiv and v). However, substitution of wtVp1 with Vp1BR3Δ (Vp1BR3Δ/Vp3) resulted in noninfectious virions (Fig.5Avi). The phospholipase domain of Vp1BR3Δ is functional based on in vitro assay (data not shown), supporting the premise that BR3 plays a primary role in virion transport to the nucleus. To further illustrate this point, AAV2 virions composed of wtVp2, wtVp3, and mutant Vp1 (Vp1BR3Δ) were infectious (Fig.5Avii). Vp1BR3Δ/Vp2/Vp3 infectious virions supports the premise that functional phospholipase activity is contributed by the mutant Vp1 subunit (Vp1BR3Δ) and further suggests that the redundant BR3 domain on Vp2 is also functional, allowing the transport of viral genomes into the nucleus. Similar GFP transduction data were collected in the presence or absence of Ad, suggesting that the trafficking helper functions of Ad (64) do not aid in BR3Δ genome import into the nucleus compared to the wt. Previous studies have suggested that the role of Vp2 is unknown and dispensable (57). Our data support the potential for the BR3 region in either Vp1 or Vp2 or both to facilitate nuclear transport of incoming virions/viral genomes into the nucleus. It has been previously identified that Vp1 N termini can become surface exposed when capsids are heated, suggesting that this may be mimicking what is happening within the cell to expose the phospholipase domain of Vp1 (2, 4). Figure 5B adds to the previous studies by showing (utilizing MAb A69 specific to Vp2 N terminus) that the N termini of Vp2 can also become surface exposed on the virion (composed of Vp2/Vp3) after a mild heat treatment. This suggests that when the necessary capsid conformational change occurs within the cell, Vp2 N termini may also become surface exposed, aiding in infectivity.

BR4 may be a region in the capsid subunit that is important for virion assembly. As depicted in Fig. 1A, BR4 is located in the Vp3 coding region. When this region is mutagenized, DNase-resistant particles are not detected by dot blot hybridization, suggesting that capsids are not assembled. After obtaining this result, we carried out additional studies to help determine the underlying defect of BR4 in AAV infection. We fractionated transfected 293 cells into nuclear and cytoplasmic

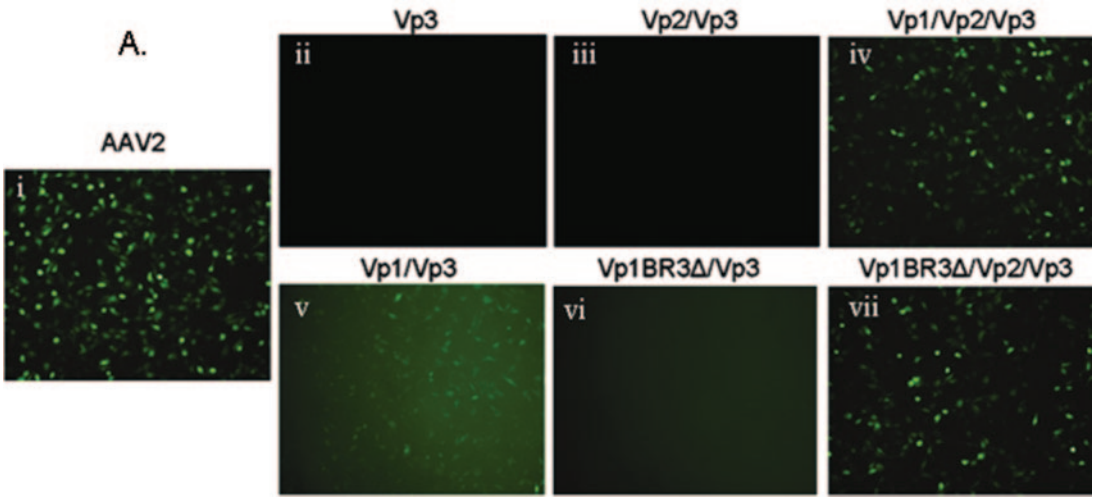

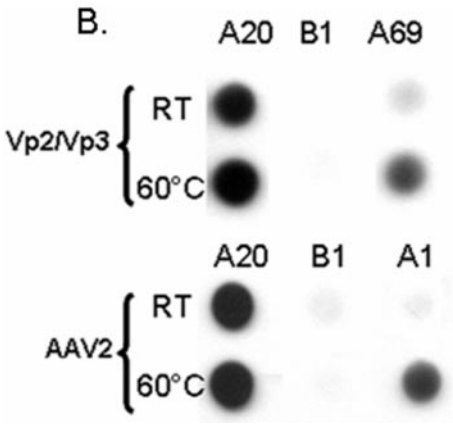

FIG. 5. (A) Fluorescence microscopy images of HeLa cells infected with assorted AAV2 virions in the presence of adenovirus at an MOI of 5. HeLa cells were infected with AAV2 (i), Vp3 only (ii), Vp2/Vp3 (iii), Vp1/Vp2/Vp3 (iv), Vp1/Vp3 (v), Vp1BR3Δ/Vp3 (vi), and Vp1BR3Δ/Vp2/Vp3 (vii) GFP viruses at 3,000 viral genomes/cell to determine whether the redundant BR3 sequence on Vp2 is functional. AAV2 was produced from a single helper plasmid supplying all three capsid proteins. The Vp2/Vp3 virus was produced from the Vp2/Vp3 expressing plasmid. The Vp1 only, Vp1BR3Δ only, and Vp3 only expressing plasmids were produced for the present study by mutating the start codons of Vp2/Vp3 and Vp1/Vp2, respectively. These plasmids were then utilized together and in combination with the Vp2/Vp3 plasmid to produce the Vp1/Vp2/Vp3, Vp1BR3Δ/Vp2/Vp3, Vp1/Vp3, and Vp1BR3Δ/Vp3 viruses. (B) A native dot blot assay of wtAAV2 and Vp2/Vp3 virions. Each virus was heated to 60°C for 5 min and then reacted with A20 (intact capsids), B1 (unassembled capsids), A1 (Vp1 N termini), or A69 (Vp1 and Vp2 N termini) under nondenaturing conditions.

fractions at 24 h posttransfection and immunoprecipitated them with B1 and A20 antibodies that recognize unassembled and assembled capsids, respectively. Based on Western blot analysis, capsid proteins were immunoprecipitated from the cytoplasm and nuclear fractions for both wt and BR4 mutants (Fig. 1C, lanes 4 to 7). However, assembled capsids were only detected from the nucleus with wt capsid subunits after A20 immunoprecipitation (Fig. 1C, lanes 2 and 3). Altogether, these data suggest that BR4 capsid proteins are produced at concentrations similar to those for wt and are able to access the nucleus but do not assemble into intact virions.

Previous studies have established that AAV2 assembles in the nucleus in "intranuclear assembly centers" that increase in size over time as more capsid proteins enter and virions are assembled (23, 59, 60). It has been suggested that the assembly centers occur within nucleoli (59). A number of other viruses or viral components have been shown to interact with the nucleolus and its components, supporting the logic for this observation (10, 21, 34, 36–38, 42, 63). With this evidence in hand, we set up an immunofluorescence study to determine whether intranuclear assembly centers form in the nuclei of pACG2-BR4Δ-transfected HeLa cells. HeLa cells were coinfected with wtAAV2 and adenovirus as a control, along with independent transfections of wt AAV2 plasmid pACG2 and pACG2-BR4Δ, as described in Materials and Methods. Cells were fixed and probed with the B1 antibody and fibrillarin antibody (specific for nucleoli). The results from this analysis established that intranuclear assembly centers are present in wtAAV2-infected cells, as previously described (23, 59, 60), along with wt and mutant BR4Δ transfected cells (Fig. 6A, C, and E). DAPI staining was carried out on all samples to confirm the nuclear location of the assembly centers (Fig. 6B, D, and F). However, similar foci were also detected in the cytoplasm of pACG2-BR4Δ transfected cells (Fig. 6E, white boxed regions), suggesting that mutagenesis of this region affects the localization of capsid subunits. Further analysis of the BR4 mutation with respect to the crystal structure of AAV2 suggests potential destabilization of the capsid subunit structure by abrogating essential hydrogen bonding from the adjacent beta strand that might lead to possible precipitation in the cytoplasm.

DISCUSSION

Successful infection by AAV is a multipart process involving specific interaction of the virion at the surface of the cell, entry via an endocytic pathway, and escape from this compartment into the cytoplasm from which the viral genome is delivered to the nucleus of the cell (5). Specific domains on and within the capsid are necessary to carry out the infectious process, includ-

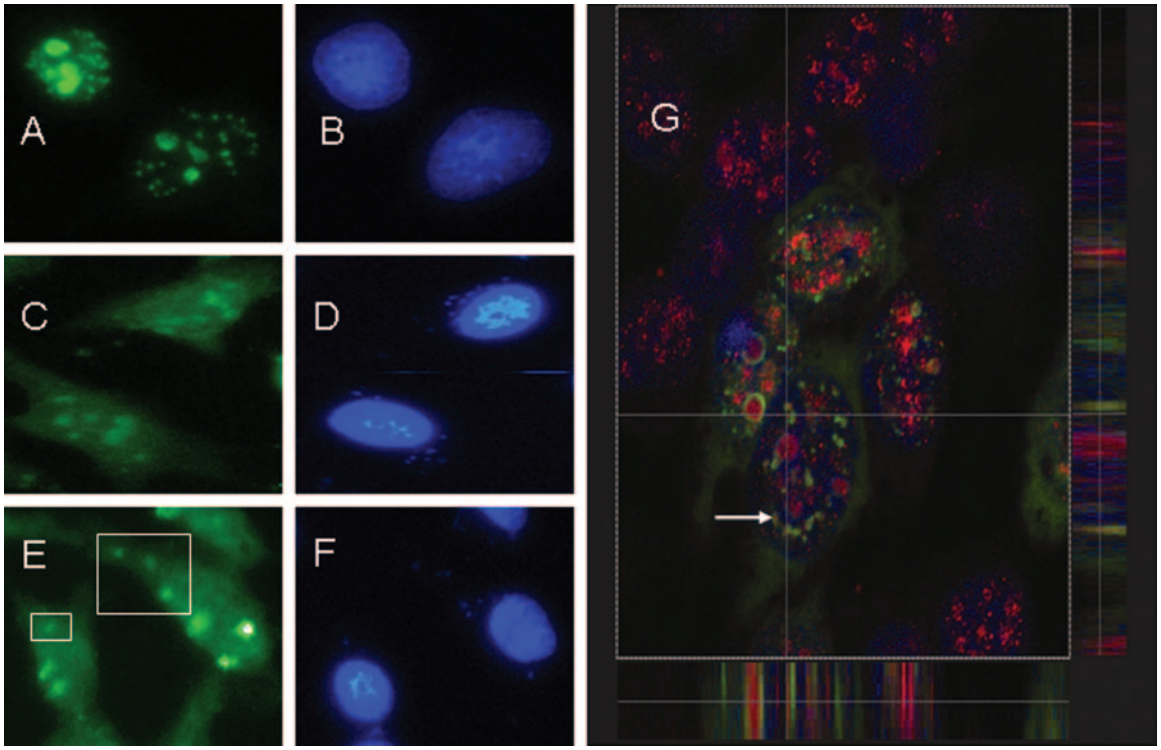

FIG. 6. Immunofluorescence and confocal microscopy images of HeLa cells infected with wtAAV2 and transfected with pACG2 and pACG2-BR4Δ. Panels A through F were analyzed by indirect immunofluorescence using a Leitz DMIL fluorescence microscope. Panel G is an overlay image that was analyzed by confocal microscopy using the Leica SP2 aobs confocal microscope. HeLa cells were infected with wtAAV2 and adenovirus (A and B), transfected with pACG2 and adenovirus helper plasmid XX680 (C and D), and transfected with pACG2-BR4Δ (E and F) and adenovirus helper plasmid. Each sample was probed with primary antibodies B1 (anti-capsid subunits) and fibrillarin (nucleolar protein). Capsid proteins are identified by green fluorescence (Alexa-Fluor 488 secondary) (A, C, and E), fibrillarin is identified by red fluorescence (Alexa-Fluor 568) (G), and nuclei are identified by blue fluorescence (DAPI) (B, D, F, and G). A series of horizontal sections (each 0.3 μm) were obtained for panel G. The white arrow points to intranuclear assembly centers identified by the B1 antibody. GFP exposure times were identical for panels C and E, while a shorter exposure time was used for panel B due to increased abundance of capsid protein in the cells.

ing domains essential for receptor binding and internalization, endosome escape, and nuclear transport (1, 27, 40, 64). At present, little is known about the later steps in the AAV infection pathway. From the limited studies to date, a discrepancy regarding these steps exists, and recent studies suggest that trafficking can be a function of the cell type studied (1, 7–9, 18–20, 48, 49, 64). We set out here to delineate BRs (typically associated with NLS activity) on the AAV capsid that are essential for viral infectivity and nuclear accumulation of capsid proteins for virion assembly. Four BRs representing potential NLS domains were identified in the capsid of AAV2 and mutagenized to determine their respective roles in the life cycle of AAV2. AAV2 with mutated forms of each BR were assessed for their ability to produce virus, incorporate all three capsid proteins within the virion at wt ratios, and transduce cells and were assayed for capsid protein distribution in cells actively producing the virus (BR4). We show that BR3 and BR4, as depicted in Fig. 1A, were essential for viral infectivity and capsid assembly, respectively.

A nuclear targeting sequence is essential for AAV infection. The size of the AAV capsid is 25 nm, which is close to the functional capacity limit of the nuclear pore complex (11). Therefore, AAV could potentially enter the nucleus via the NPC as an intact particle. It is unknown whether AAV enters the nucleus intact or disassembles perinuclearly. Evidence supporting both possibilities has been uncovered (1, 35, 48, 64). Based on structural studies, the putative NLS region (BR3) is located within the virion on the N terminus of Vp2 and Vp1 and therefore could not be used by an incoming virion to interact with the NPC transport machinery unless conformational changes took place first (28, 29, 61, 65). However, the data from our study suggest that the BR3 sequence is necessary for AAV2 to deliver its genome within the nucleus and subsequently transduce the cells (Fig. 3, 5, 6, and 7). A working model for how autonomous parvoviruses resolve this concern has been established, and most likely is mimicked to some degree by AAV. Specifically, it has been shown that MVM and CPV virions expose their NLS-containing Vp1 N termini in vitro upon exposure to mild heating or low pH without disassembly, mimicking what might be occurring within the cell, presumably in the endosome (3, 4, 46, 51, 56). Two recent studies have shown that Vp1 is located within the AAV virion (2, 28). We show in the present study that Vp2 is also exposed after mild heating (Fig. 5B). Thus, the AAV capsid must undergo a certain degree of conformational change or partial disassembly during intracellular trafficking to the nucleus, leading to the exposure of the N-terminal 172 amino acids of Vp1 and/or the N-terminal 35 amino acids of Vp2, exposing the

BR3 domain (Fig. 5B). The availability of BR3 would then aid in nuclear targeting of the incoming virion.

The BR3 sequence represents a region on the capsid important for AAV2 infectivity and is functional on Vp1 and Vp2 capsid proteins. As described earlier, the BR3 sequence was previously proposed as a mediator for targeting individual capsid proteins to the nucleus during progeny virion assembly, and this transport was facilitated by Vp2 (22). This conclusion does not seem to be likely or the sole function based on the facts that the Vp2 concentration is much lower (ca. 10- to 20-fold) than Vp3 and that previous studies have demonstrated the ability to produce Vp3 only particles at or near wt levels (data not shown) (57). In the present study, we analyzed BR3 in the context of the virus and found it to be essential for AAV2 infectivity (Fig. 2, 3, 4, and 5A) but not necessary for the localization of capsid proteins to the nucleus during viral assembly (Fig. 1B). Substitution of the BR3 sequence with the NLS identified for CPV, PAKRARR (55, 56), was found to confer NLS function in the context of the rAAV2 virion, adding further support that this basic amino acid region located in Vp1 and Vp2 is essential for primary infection (Fig. 4). It will be of interest to determine whether BR3 interacts with any known nuclear transport factors or acts solely as an NLS for virion nuclear transport.

In accordance with identifying the role of BR3 as the NLS important for infectivity, we sought to determine whether the function of the BR3 sequence, which resides in both Vp1 and Vp2, is redundant between these two capsid proteins. To address this concern, we produced rAAV2 composed of single components or combinations of capsid subunits (Vp3 only, Vp1/Vp3, Vp1BR3Δ/Vp3, Vp2/Vp3, and Vp1BR3Δ/Vp2/Vp3) encapsidating the eGFP transgene. As illustrated in Fig. 5A, we demonstrated a requirement for Vp2BR3 in a virion background lacking this motif in Vp1. This virion combination was infectious, suggesting that the BR3 sequence on Vp2 is also functional and redundant to the BR3 provided by Vp1 in wt virions. Consistent with our mutant combination virion studies, our in vitro heating data suggest that the N terminus of Vp2 can be exposed in a manner similar to that of Vp1, supporting a role for Vp2 in the infectious pathway (Fig. 5B).

The BR4 domain may play a role in virion assembly. Our initial studies done on each of the BR mutants illustrated that BR4Δ did not produce intact particles but was capable of producing capsid subunits that accessed the nucleus (Fig. 1C), localizing in intranuclear assembly centers (Fig. 6E and F) (32, 33). It is noteworthy to mention that two studies have suggested that AAV virion assembly occurs in nucleoli utilizing indirect immunofluorescence for nucleolin (44) and an unspecified nucleolar protein (59). However, utilizing confocal microscopy (Fig. 6G and data not shown), the intranuclear assembly centers do not colocalize with nucleoli (based on the fibrillarin staining), suggesting that these capsid assembly centers are distinct from nucleoli as previously described (23a). In line with this, two studies have shown that adenovirus is capable of redistributing nucleolar proteins such as nucleolin, B23, and fibrillarin to other regions of the cell, including the cytoplasm (37, 41). Adenovirus coinfection was used in all of the AAV subcellular localization studies, including the present study, suggesting that this result may be an artifact of adenovirus in the cell.

The present study also revealed that the BR4Δ capsid proteins were produced at levels similar to those of the wt capsid proteins and accumulated in the nucleus and cytoplasm similarly to wt (Fig. 1C). However, intact particles were not detected in the nucleus of pACG2-BR4Δ transfected cells, which is in contrast to pACG2-wt transfected cells (Fig. 1C, lanes 2 and 3). Based on these data, the linear motif of BR4 does not seem to be the domain essential for subunit entry into the nucleus or important for localizing capsid subunits into the intranuclear assembly centers. However, if similar to autonomous parvovirus (MVM), a conformational/structural (three-dimensional) NLS, formed from capsid subunit interactions, may be essential to access to the nucleus for assembly. In fact, further analysis into the crystal structure of AAV2 suggests that mutagenesis of residues K309 and R310 to asparagine may destabilize the structure of the capsid subunit and may not be involved in capsid subunit nuclear import (M. Agbandje-McKenna, unpublished data) as depicted in Fig. 7B. These two residues are located in beta strand D, which is a core structural motif that is located within the capsid of parvoviruses. K309 and R310 directly interact (through hydrogen bonding) with E683 and E685, respectively, in the adjacent beta strand I. Changing K309 and R310 to asparagines disrupts these interactions. This premise is supported by an independent study showing a similar phenotype when E683 and E685 were mutated to alanine (62). These two independent studies show similar results, which suggests a possible trafficking defect or defect in intersubunit interactions as a consequence of misfolding.

Infectious entry pathway of AAV2. Figure 7 is a schematic representation of the infectious entry pathway of AAV2 based on previous studies and in conjunction with the data described here. The early steps of AAV2 infection begin with attachment to a variety of cell surface receptors, such as HSPG, FGFR, $\alpha_v\beta_5$ integrin, and hepatocyte growth factor receptor (c-Met) (Fig. 7, step 1) (6, 26, 43, 52, 53) followed by clathrin-mediated endocytosis (Fig. 7 step 2). Based on a number of studies, it has been proposed that AAV requires endosomal acidification to escape from the late endosome and traffic to the nucleus (Fig. 7, steps 3 and 4) (7, 19, 66, 67). The data based on autonomous parvoviruses suggest that, prior to escaping the endosome, the virion undergoes conformational changes, leading to the exposure of the N terminus of Vp1, which is necessary for escape (Fig. 7, step 3) (3, 46). However, based on endosomal pH studies on CPV infection, the exposure of Vp1 may not be the only factor involved in escape from the endosome (51). Our data suggest that BR3, located 172 amino acids in Vp1 and 35 amino acids in Vp2, must also be exposed (Fig. 5B) at some point in the infectious pathway, presumably the endosome, for a successful infection to occur (Fig. 7, step 3 image enhanced). It was determined that AAV capsids are ubiquitinated, marking them for degradation by the proteasome (Fig. 7, step 5) (66). In support of this, the use of proteasome inhibitors such as MG-132 and LLnL has been shown to increase transduction, providing evidence that, after endosome escape, AAV must elude cytoplasmic proteasomes while trafficking to the nucleus (Fig. 7, steps 4 and 5) (7, 67) or facilitating downstream steps such as uncoating or gene expression, etc. It remains unclear whether the entry of intact AAV2 into the

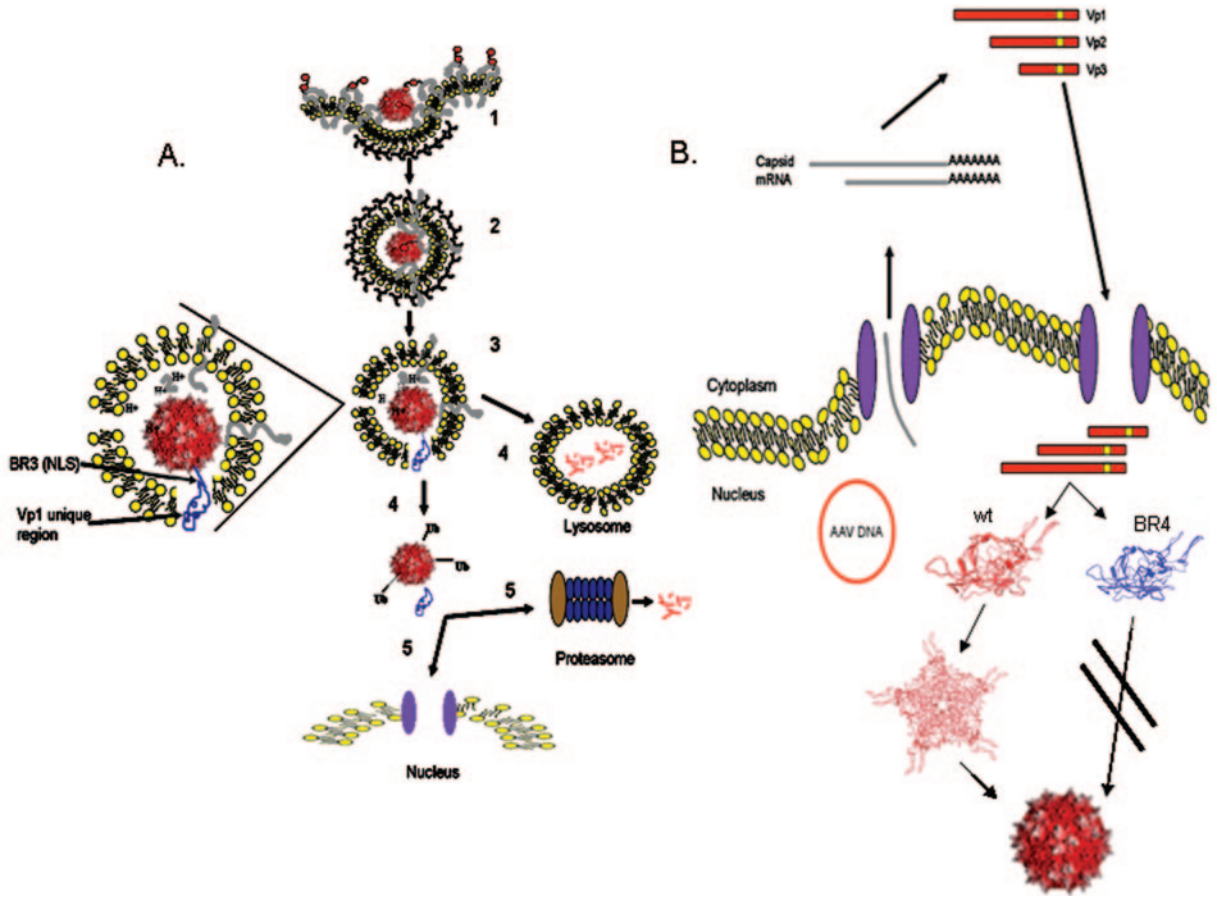

FIG. 7. (A) Schematic representation of the infectious entry pathway of AAV2 (step 1). The first step in AAV2 infection is binding to its primary receptor and a secondary receptor (step 2). AAV2 enters the cell by endocytosis via clathrin-coated pits and is brought into the cytoplasm in an early endosome (step 3). The early endosome then matures into a late endosome as the pH begins to drop to around 5. A pH-dependent conformational change occurs that is thought to expose the N terminus of Vp1, and possibly BR3, providing the phospholipase activity for endosome escape and region essential for genome import into the nucleus (step 4). At this point in the pathway, AAV either fails to escape the late endosome, where it later becomes degraded by the lysosome or escapes into the cytoplasm perinuclearly, where it becomes ubiquitinated (step 5). The ubiquitinated virions can then be recognized by cytoplasmic proteasomes on their way to the nucleus, where they are degraded, but those that avoid interaction with the proteasomes continue on their path to the nucleus (step 5). (B) Schematic representation of the pathway involved in AAV2 capsid protein synthesis and assembly of wt capsid proteins and those containing the BR4 mutation. AAV DNA is found in the nucleus of transfected cells, and mRNA is produced and translated into the capsid proteins, which shuttle into the nucleus for assembly. The red capsid proteins represent wt capsid sequence, while the blue proteins represent the capsid proteins with the BR4 mutations (depicted in yellow). The wt capsid subunits are capable of intersubunit interactions, leading to the intermediate pentamer/trimer formation, leading to capsid assembly. We propose that the misfolded/destabilized BR4 capsid subunits are incapable of intersubunit interactions and cannot form intact virions.

nucleus occurs or whether uncoating occurs before or during nuclear entry (35, 64).

We have shown that the putative NLS of AAV2, identified by Hoque et al. and termed BR3 here, is not solely necessary to mediate the nuclear accumulation of capsid proteins for nuclear assembly but is important in the translocation of the AAV2 genome across the nuclear envelope during primary infection. We suggest that BR3 is a putative NLS necessary for AAV infection. The BR3 domain is also conserved among AAV serotypes 1 through 11 (Table 1), suggesting that each serotype accesses the nucleus utilizing a similar NLS. The Vp1/Vp2-specific BR3 sequence is similar to consensus sequences that bind karyopherin α and β receptors (24, 25), suggesting that AAV may use components of this transport pathway to bind or dock their genomes to the NPC in associ-

TABLE 1. Sequences of AAV serotypes 1 to 11

AAV	Sequence	
	BR3 domain	BR4 domain
AAV2	PARKRLNF	RPKRLN
AAV1	PAKKRLNF	RPKRLN
AAV3	PARKRLNF	RPKKLS
AAV4	PAKKKLVF	RPKAMR
AAV5	PKRKKART	RPRSLR
AAV6	PAKKRLNF	RPKRLN
AAV7	PARKRLNF	RPKKLR
AAV8	PARKRLNF	RPKRLS
AAV9	PAKKRLNF	RPKRLN
AAV10	PAKKRLNF	RPKRLS
AAV11	PARKRLNF	RPKAMR

ation with Vp1 and/or Vp2. Numerous different forms of α and β importins exist in eukaryotic cells (in different concentrations), suggesting that different isoforms could bind particular target proteins. Substitution of the CPV NLS for BR3 in AAV2 was able to carry out a successful infection, implying that it may be possible to substitute well-characterized NLSs for BR3 to enhance transduction in a cell-specific manner. This study also suggests that Vp2 may play a role in the life cycle of AAV, and this function may be most evident in vivo such as enhancing transduction. It is clear that a better understanding of AAV biology, such as the role of NLS domains, holds promise for improving AAV vectors by modifying capsid structure to obtain virion infectivity with desired traits (i.e., efficient trafficking, enhanced nuclear targeting, and/or timely release of vector template in the nucleus).

ACKNOWLEDGMENTS

We thank Michael Chua of the University of North Carolina at Chapel Hill Michael Hooker Microscopy Facility for assistance in our microscopy studies.

This study was supported by NIH research grants 5 P01 GM059299, 2 P01 HL051818, P30 DK065988-01, 5 P01 HL066973, and 5 P30 DK34987.

REFERENCES

1. **Bartlett, J. S., R. Wilcher, and R. J. Samulski.** 2000. Infectious entry pathway of adeno-associated virus and adeno-associated virus vectors. J. Virol. **74:** 2777–2785.
2. **Bleker, S., F. Sonntag, and J. A. Kleinschmidt.** 2005. Mutational analysis of narrow pores at the fivefold symmetry axes of adeno-associated virus type 2 capsids reveals a dual role in genome packaging and activation of phospholipase A2 activity. J. Virol. **79:**2528–2540.
3. **Carreira, A., M. Menendez, J. Reguera, J. M. Almendral, and M. G. Mateu.** 2004. In vitro disassembly of a parvovirus capsid and effect on capsid stability of heterologous peptide insertions in surface loops. J. Biol. Chem. **279:**6517–6525.
4. **Cotmore, S. F., A. M. D'Abramo, Jr., C. M. Ticknor, and P. Tattersall.** 1999. Controlled conformational transitions in the MVM virion expose the VP1 N terminus and viral genome without particle disassembly. Virology **254:**169–181.
5. **Ding, W., L. Zhang, Z. Yan, and J. F. Engelhardt.** 2005. Intracellular trafficking of adeno-associated viral vectors. Gene Ther. **12:**873–880.
6. **Di Pasquale, G., B. L. Davidson, C. S. Stein, I. Martins, D. Scudiero, A. Monks, and J. A. Chiorini.** 2003. Identification of PDGFR as a receptor for AAV-5 transduction. Nat. Med. **9:**1306–1312.
7. **Douar, A. M., K. Poulard, D. Stockholm, and O. Danos.** 2001. Intracellular trafficking of adeno-associated virus vectors: routing to the late endosomal compartment and proteasome degradation. J. Virol. **75:**1824–1833.
8. **Duan, D., Q. Li, A. W. Kao, Y. Yue, J. E. Pessin, and J. F. Engelhardt.** 1999. Dynamin is required for recombinant adeno-associated virus type 2 infection. J. Virol. **73:**10371–10376.
9. **Duan, D., Y. Yue, Z. Yan, J. Yang, and J. F. Engelhardt.** 2000. Endosomal processing limits gene transfer to polarized airway epithelia by adeno-associated virus. J. Clin. Investig. **105:**1573–1587.
10. **Dundr, M., G. H. Leno, M. L. Hammarskjold, D. Rekosh, C. Helga-Maria, and M. O. Olson.** 1995. The roles of nucleolar structure and function in the subcellular location of the HIV-1 Rev. protein. J. Cell Sci. **108**(Pt. 8)**:**2811–2823.
11. **Feldherr, C. M., E. Kallenbach, and N. Schultz.** 1984. Movement of a karyophilic protein through the nuclear pores of oocytes. J. Cell Biol. **99:** 2216–2222.
12. **Fu, Z., T. Chakraborti, S. Morse, G. S. Bennett, and G. Shaw.** 2001. Four casein kinase I isoforms are differentially partitioned between nucleus and cytoplasm. Exp. Cell Res. **269:**275–286.
13. **Girod, A., C. E. Wobus, Z. Zadori, M. Ried, K. Leike, P. Tijssen, J. A. Kleinschmidt, and M. Hallek.** 2002. The VP1 capsid protein of adeno-associated virus type 2 is carrying a phospholipase A2 domain required for virus infectivity. J. Gen. Virol. **83:**973–978.
14. **Greber, U. F., M. Suomalainen, R. P. Stidwill, K. Boucke, M. W. Ebersold, and A. Helenius.** 1997. The role of the nuclear pore complex in adenovirus DNA entry. EMBO J. **16:**5998–6007.
15. **Grieger, J. C., and R. J. Samulski.** 2005. Packaging capacity of adeno-associated virus serotypes: impact of larger genomes on infectivity and postentry steps. J. Virol. **79:**9933–9944.
16. **Haberman, R. P., T. J. McCown, and R. J. Samulski.** 2000. Novel transcriptional regulatory signals in the adeno-associated virus terminal repeat A/D junction element. J. Virol. **74:**8732–8739.

16a. **Haberman, R., G. Kroner-Lux, et al.** 1999. Production of recombinant adeno-associated virus vectors. John Wiley & Sons, Inc., New York, N.Y.

17. **Hall, M. N., L. Hereford, and I. Herskowitz.** 1984. Targeting of *Escherichia coli* β-galactosidase to the nucleus in yeast. Cell **36:**1057–1065.
18. **Hansen, J., K. Qing, H. J. Kwon, C. Mah, and A. Srivastava.** 2000. Impaired intracellular trafficking of adeno-associated virus type 2 vectors limits efficient transduction of murine fibroblasts. J. Virol. **74:**992–996.
19. **Hansen, J., K. Qing, and A. Srivastava.** 2001. Adeno-associated virus type 2-mediated gene transfer: altered endocytic processing enhances transduction efficiency in murine fibroblasts. J. Virol. **75:**4080–4090.
20. **Hansen, J., K. Qing, and A. Srivastava.** 2001. Infection of purified nuclei by adeno-associated virus 2. Mol. Ther. **4:**289–296.
21. **Hiscox, J. A., T. Wurm, L. Wilson, P. Britton, D. Cavanagh, and G. Brooks.** 2001. The coronavirus infectious bronchitis virus nucleoprotein localizes to the nucleolus. J. Virol. **75:**506–512.
22. **Hoque, M., K. Ishizu, A. Matsumoto, S. I. Han, F. Arisaka, M. Takayama, K. Suzuki, K. Kato, T. Kanda, H. Watanabe, and H. Handa.** 1999. Nuclear transport of the major capsid protein is essential for adeno-associated virus capsid formation. J. Virol. **73:**7912–7915.
23. **Hunter, L. A., and R. J. Samulski.** 1992. Colocalization of adeno-associated virus Rep and capsid proteins in the nuclei of infected cells. J. Virol. **66:** 317–324.

23a. **Hunter, L. A.** 1992. Ph.D. thesis. University of Pittsburgh, Pittsburgh, Pa.

24. **Kalderon, D., W. D. Richardson, A. F. Markham, and A. E. Smith.** 1984. Sequence requirements for nuclear location of simian virus 40 large-T antigen. Nature **311:**33–38.
25. **Kalderon, D., B. L. Roberts, W. D. Richardson, and A. E. Smith.** 1984. A short amino acid sequence able to specify nuclear location. Cell **39:**499–509.
26. **Kashiwakura, Y., K. Tamayose, K. Iwabuchi, Y. Hirai, T. Shimada, K. Matsumoto, T. Nakamura, M. Watanabe, K. Oshimi, and H. Daida.** 2005. Hepatocyte growth factor receptor is a coreceptor for adeno-associated virus type 2 infection. J. Virol. **79:**609–614.
27. **Kern, A., K. Schmidt, C. Leder, O. J. Muller, C. E. Wobus, K. Bettinger, C. W. Von der Lieth, J. A. King, and J. A. Kleinschmidt.** 2003. Identification of a heparin-binding motif on adeno-associated virus type 2 capsids. J. Virol. **77:**11072–11081.
28. **Kronenberg, S., B. Bottcher, C. W. von der Lieth, S. Bleker, and J. A. Kleinschmidt.** 2005. A conformational change in the adeno-associated virus type 2 capsid leads to the exposure of hidden VP1 N termini. J. Virol. **79:**5296–5303.
29. **Kronenberg, S., J. A. Kleinschmidt, and B. Bottcher.** 2001. Electron cryomicroscopy and image reconstruction of adeno-associated virus type 2 empty capsids. EMBO Rep. **2:**997–1002.
30. **Lemmon, S. K., and L. M. Traub.** 2000. Sorting in the endosomal system in yeast and animal cells. Curr. Opin. Cell Biol. **12:**457–466.
31. **Li, J., R. J. Samulski, and X. Xiao.** 1997. Role for highly regulated rep gene expression in adeno-associated virus vector production. J. Virol. **71:**5236–5243.
32. **Lombardo, E., J. C. Ramirez, M. Agbandje-McKenna, and J. M. Almendral.** 2000. A beta-stranded motif drives capsid protein oligomers of the parvovirus minute virus of mice into the nucleus for viral assembly. J. Virol. **74:** 3804–3814.
33. **Lombardo, E., J. C. Ramirez, J. Garcia, and J. M. Almendral.** 2002. Complementary roles of multiple nuclear targeting signals in the capsid proteins of the parvovirus minute virus of mice during assembly and onset of infection. J. Virol. **76:**7049–7059.
34. **Lutz, P., F. Puvion-Dutilleul, Y. Lutz, and C. Kedinger.** 1996. Nucleoplasmic and nucleolar distribution of the adenovirus IVa2 gene product. J. Virol. **70:**3449–3460.
35. **Lux, K., N. Goerlitz, S. Schlemminger, L. Perabo, D. Goldnau, J. Endell, K. Leike, D. M. Kofler, S. Finke, M. Hallek, and H. Buning.** 2005. Green fluorescent protein-tagged adeno-associated virus particles allow the study of cytosolic and nuclear trafficking. J. Virol. **79:**11776–11787.
36. **MacLean, C. A., F. J. Rixon, and H. S. Marsden.** 1987. The products of gene US11 of herpes simplex virus type 1 are DNA-binding and localize to the nucleoli of infected cells. J. Gen. Virol. **68**(Pt. 7)**:**1921–1937.
37. **Matthews, D. A.** 2001. Adenovirus protein V induces redistribution of nucleolin and B23 from nucleolus to cytoplasm. J. Virol. **75:**1031–1038.
38. **Matthews, D. A., and W. C. Russell.** 1998. Adenovirus core protein V is delivered by the invading virus to the nucleus of the infected cell and later in infection is associated with nucleoli. J. Gen. Virol. **79**(Pt. 7)**:**1671–1675.
39. **Ojala, P. M., B. Sodeik, M. W. Ebersold, U. Kutay, and A. Helenius.** 2000. Herpes simplex virus type 1 entry into host cells: reconstitution of capsid binding and uncoating at the nuclear pore complex in vitro. Mol. Cell. Biol. **20:**4922–4931.
40. **Opie, S. R., K. H. Warrington, Jr., M. Agbandje-McKenna, S. Zolotukhin, and N. Muzyczka.** 2003. Identification of amino acid residues in the capsid proteins of adeno-associated virus type 2 that contribute to heparan sulfate proteoglycan binding. J. Virol. **77:**6995–7006.

41. **Puvion-Dutilleul, F., and M. E. Christensen.** 1993. Alterations of fibrillarin distribution and nucleolar ultrastructure induced by adenovirus infection. Eur. J. Cell Biol. **61:**168–176.
42. **Pyper, J. M., J. E. Clements, and M. C. Zink.** 1998. The nucleolus is the site of Borna disease virus RNA transcription and replication. J. Virol. **72:**7697–7702.
43. **Qing, K., C. Mah, J. Hansen, S. Zhou, V. Dwarki, and A. Srivastava.** 1999. Human fibroblast growth factor receptor 1 is a coreceptor for infection by adeno-associated virus 2. Nat. Med. **5:**71–77.
44. **Qiu, J., and K. E. Brown.** 1999. A 110-kDa nuclear shuttle protein, nucleolin, specifically binds to adeno-associated virus type 2 (AAV-2) capsid. Virology **257:**373–382.
45. **Rabinowitz, J. E., W. Xiao, and R. J. Samulski.** 1999. Insertional mutagenesis of AAV2 capsid and the production of recombinant virus. Virology **265:**274–285.
46. **Reguera, J., A. Carreira, L. Riolobos, J. M. Almendral, and M. G. Mateu.** 2004. Role of interfacial amino acid residues in assembly, stability, and conformation of a spherical virus capsid. Proc. Natl. Acad. Sci. USA **101:**2724–2729.
47. **Ryabov, E. V., S. H. Kim, and M. Taliansky.** 2004. Identification of a nuclear localization signal and nuclear export signal of the umbraviral long-distance RNA movement protein. J. Gen. Virol. **85:**1329–1333.
48. **Sanlioglu, S., P. K. Benson, J. Yang, E. M. Atkinson, T. Reynolds, and J. F. Engelhardt.** 2000. Endocytosis and nuclear trafficking of adeno-associated virus type 2 are controlled by rac1 and phosphatidylinositol-3 kinase activation. J. Virol. **74:**9184–9196.
49. **Seisenberger, G., M. U. Ried, T. Endress, H. Buning, M. Hallek, and C. Brauchle.** 2001. Real-time single-molecule imaging of the infection pathway of an adeno-associated virus. Science **294:**1929–1932.
50. **Sodeik, B., M. W. Ebersold, and A. Helenius.** 1997. Microtubule-mediated transport of incoming herpes simplex virus 1 capsids to the nucleus. J. Cell Biol. **136:**1007–1021.
51. **Suikkanen, S., M. Antila, A. Jaatinen, M. Vihinen-Ranta, and M. Vuento.** 2003. Release of canine parvovirus from endocytic vesicles. Virology **316:**267–280.
52. **Summerford, C., J. S. Bartlett, and R. J. Samulski.** 1999. AlphaVbeta5 integrin: a coreceptor for adeno-associated virus type 2 infection. Nat. Med. **5:**78–82.
53. **Summerford, C., and R. J. Samulski.** 1998. Membrane-associated heparan sulfate proteoglycan is a receptor for adeno-associated virus type 2 virions. J. Virol. **72:**1438–1445.
54. **Trotman, L. C., N. Mosberger, M. Fornerod, R. P. Stidwill, and U. F. Greber.** 2001. Import of adenovirus DNA involves the nuclear pore complex receptor CAN/Nup214 and histone H1. Nat. Cell Biol. **3:**1092–1100.
55. **Vihinen-Ranta, M., L. Kakkola, A. Kalela, P. Vilja, and M. Vuento.** 1997. Characterization of a nuclear localization signal of canine parvovirus capsid proteins. Eur. J. Biochem. **250:**389–394.
56. **Vihinen-Ranta, M., D. Wang, W. S. Weichert, and C. R. Parrish.** 2002. The VP1 N-terminal sequence of canine parvovirus affects nuclear transport of capsids and efficient cell infection. J. Virol. **76:**1884–1891.
57. **Warrington, K. H., Jr., O. S. Gorbatyuk, J. K. Harrison, S. R. Opie, S. Zolotukhin, and N. Muzyczka.** 2004. Adeno-associated virus type 2 VP2 capsid protein is nonessential and can tolerate large peptide insertions at its N terminus. J. Virol. **78:**6595–6609.
58. **Whittaker, G. R., M. Kann, and A. Helenius.** 2000. Viral entry into the nucleus. Annu. Rev. Cell Dev. Biol. **16:**627–651.
59. **Wistuba, A., A. Kern, S. Weger, D. Grimm, and J. A. Kleinschmidt.** 1997. Subcellular compartmentalization of adeno-associated virus type 2 assembly. J. Virol. **71:**1341–1352.
60. **Wistuba, A., S. Weger, A. Kern, and J. A. Kleinschmidt.** 1995. Intermediates of adeno-associated virus type 2 assembly: identification of soluble complexes containing Rep and Cap proteins. J. Virol. **69:**5311–5319.
61. **Wobus, C. E., B. Hugle-Dorr, A. Girod, G. Petersen, M. Hallek, and J. A. Kleinschmidt.** 2000. Monoclonal antibodies against the adeno-associated virus type 2 (AAV-2) capsid: epitope mapping and identification of capsid domains involved in AAV-2-cell interaction and neutralization of AAV-2 infection. J. Virol. **74:**9281–9293.
62. **Wu, P., W. Xiao, T. Conlon, J. Hughes, M. Agbandje-McKenna, T. Ferkol, T. Flotte, and N. Muzyczka.** 2000. Mutational analysis of the adeno-associated virus type 2 (AAV2) capsid gene and construction of AAV2 vectors with altered tropism. J. Virol. **74:**8635–8647.
63. **Wurm, T., H. Chen, T. Hodgson, P. Britton, G. Brooks, and J. A. Hiscox.** 2001. Localization to the nucleolus is a common feature of coronavirus nucleoproteins, and the protein may disrupt host cell division. J. Virol. **75:**9345–9356.
64. **Xiao, W., K. H. Warrington, Jr., P. Hearing, J. Hughes, and N. Muzyczka.** 2002. Adenovirus-facilitated nuclear translocation of adeno-associated virus type 2. J. Virol. **76:**11505–11517.
65. **Xie, Q., W. Bu, S. Bhatia, J. Hare, T. Somasundaram, A. Azzi, and M. S. Chapman.** 2002. The atomic structure of adeno-associated virus (AAV-2), a vector for human gene therapy. Proc. Natl. Acad. Sci. USA **99:**10405–10410.
66. **Yan, Z., R. Zak, G. W. Luxton, T. C. Ritchie, U. Bantel-Schaal, and J. F. Engelhardt.** 2002. Ubiquitination of both adeno-associated virus type 2 and 5 capsid proteins affects the transduction efficiency of recombinant vectors. J. Virol. **76:**2043–2053.
67. **Yan, Z., R. Zak, Y. Zhang, W. Ding, S. Godwin, K. Munson, R. Peluso, and J. F. Engelhardt.** 2004. Distinct classes of proteasome-modulating agents cooperatively augment recombinant adeno-associated virus type 2 and type 5-mediated transduction from the apical surfaces of human airway epithelia. J. Virol. **78:**2863–2874.
68. **Zadori, Z., J. Szelei, M. C. Lacoste, Y. Li, S. Gariepy, P. Raymond, M. Allaire, I. R. Nabi, and P. Tijssen.** 2001. A viral phospholipase A2 is required for parvovirus infectivity. Dev. Cell **1:**291–302.
69. **Zolotukhin, S., B. J. Byrne, E. Mason, I. Zolotukhin, M. Potter, K. Chesnut, C. Summerford, R. J. Samulski, and N. Muzyczka.** 1999. Recombinant adeno-associated virus purification using novel methods improves infectious titer and yield. Gene Ther. **6:**973–985.